Electronic Supplementary Material (ESI) for RSC Advances.

Supplementary Information

Enhancement of hydrogen production of Cu-TiO_2 nanocomposite photocatalyst combined with broad spectrum absorption sensitizer Erythrosin B

Piyong Zhang , Ting Song, Tingting Wang, Heping Zeng*

Key Laboratory of Functional Molecular Engineering of Guangdong Province, School of Chemistry and Chemical Engineering, South China University of Technology, Guangzhou, 510641, P. R. China.

*Corresponding author. Tel.: +86-20-87112631; Fax: +86-20-87112631; E-mail: hpzeng@scut.edu.cn;

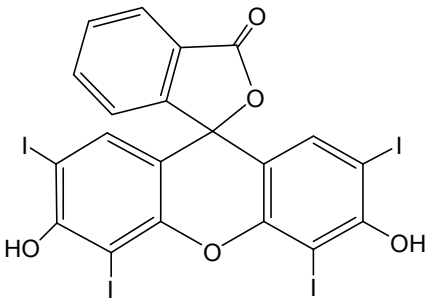

Figure S1 Structure of Erythrosin B.

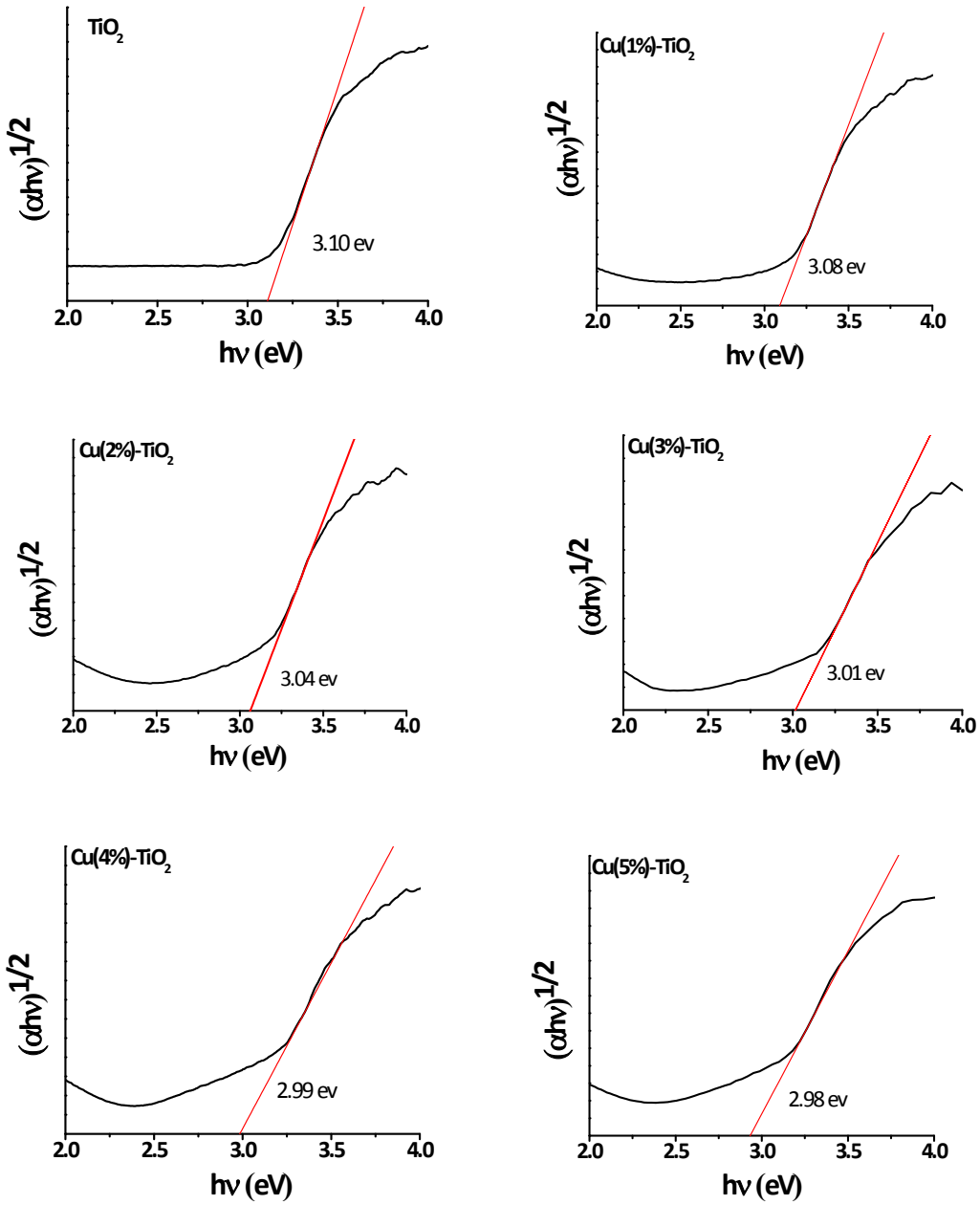

Figure S2 Tauc plots of pure TiO_2 and Cu-TiO_2 composites with different amounts of Cu.

The band gap can be estimated from the following equation:

$$\alpha h\nu = A\,(h\nu - E_g)^{n/2}$$

where α, h, ν, and E_g are the absorption coefficient, Plank's constant, light frequency, and band gap, respectively, and A is a constant. The factor n depends on the characteristics of the optical transition of a semiconductor (n = 1 for direct transition and n = 4 for indirect transition). After Cu NPs-loaded on TiO_2, the band

gap values of Cu-TiO_2 show a slight decrease, implying the scope of absorption light is broadened which is consist with UV-Vis diffuse reflectance spectra.

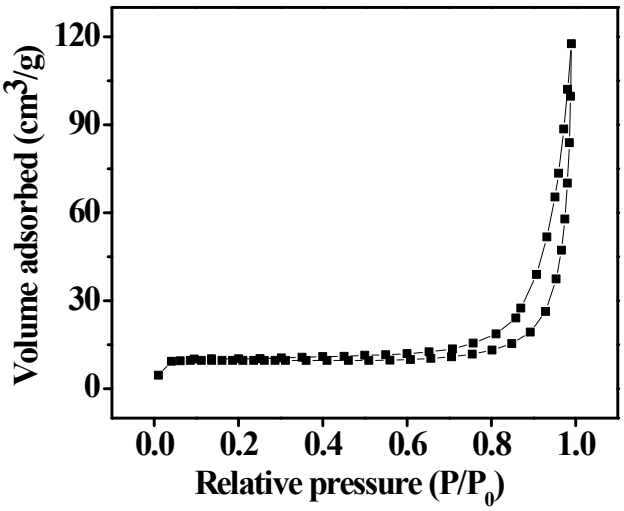

Figure S3 N_2 adsorption-desorption isotherms for TiO_2.

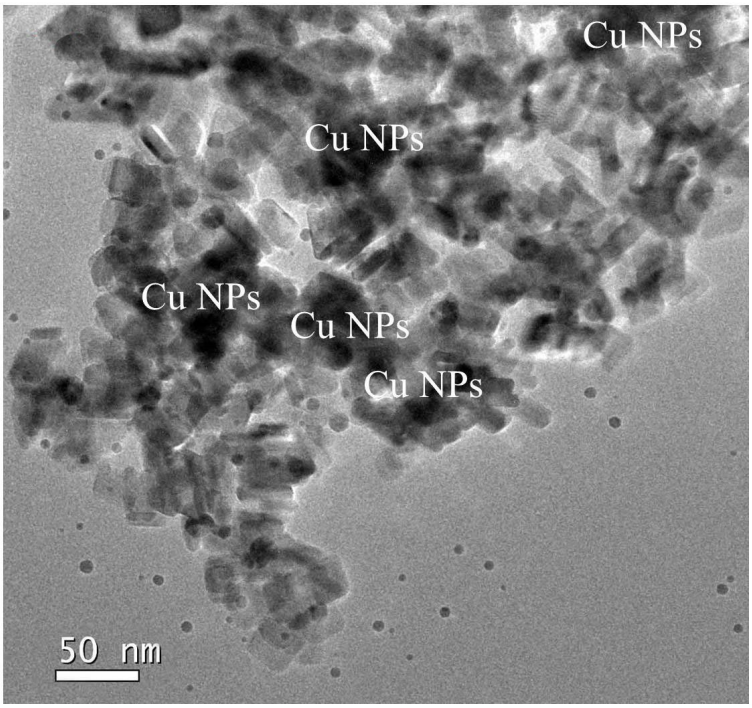

Figure S4 TEM imagine of Cu(4%)-TiO_2.

Dark-field of TEM image (Fig. S4a) indicates that Cu NPs were aggregated.

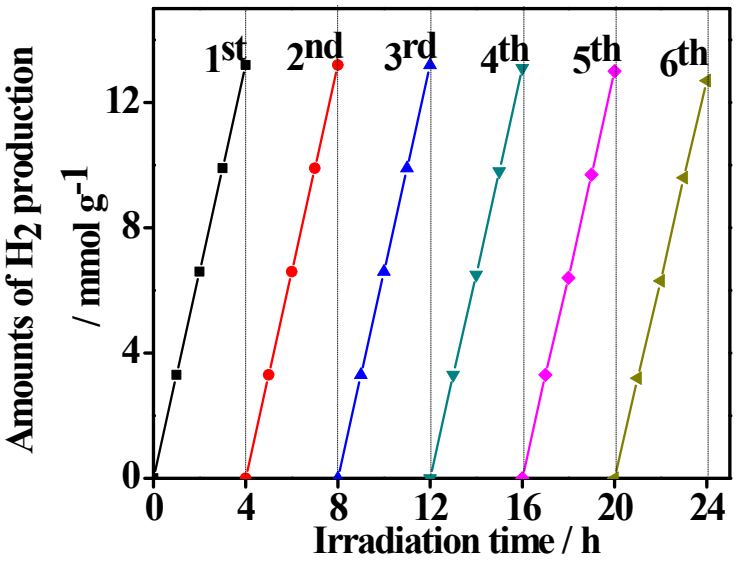

Figure S5 The cycling test of photocatalytic H_2 production for Cu(3%)-TiO_2 (irradiation time=24 h).

Little deactivation of the catalyst occurs upon repeated use, implying that it exhibits good stability and reusability.

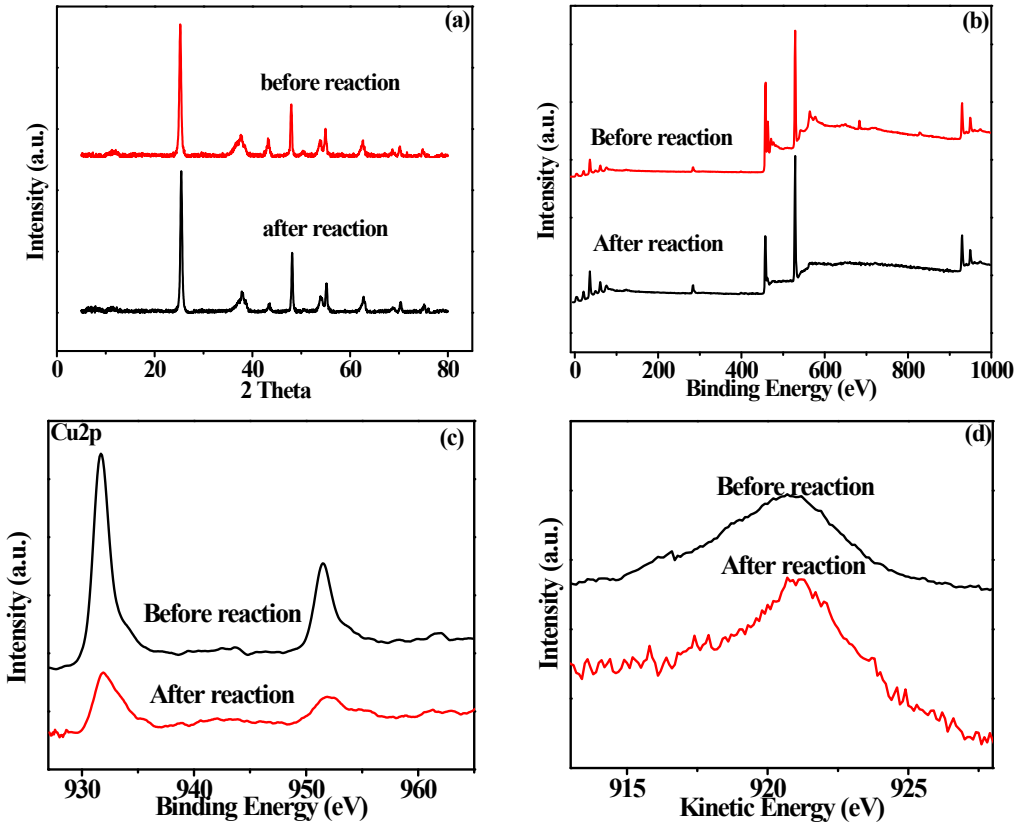

Figure S6 (a) XRD patterns and XPS spectra of Cu(3%)-TiO_2, **(b)** survey spectrum,

(c) Cu2p and **(d)** Cu LMM before and after the stability test of hydrogen production.

There are no obvious changes in the positions of the peaks, suggesting that it has considerable photostability.

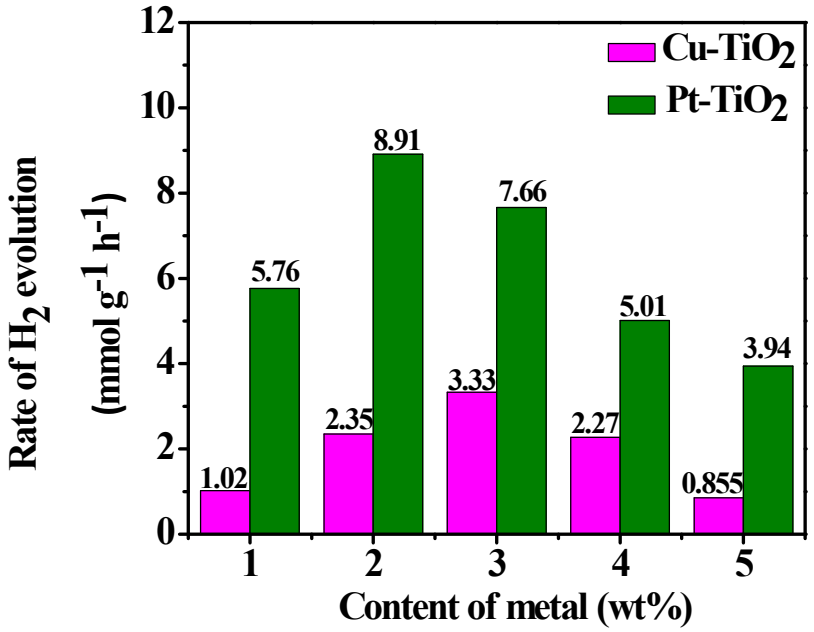

Figure S7 Photocatalytic H_2 production of Pt-TiO_2 and Cu-TiO_2 with various content of metal.

Pt-TiO_2 nanocomposites were synthesized by deposition-precipitation method, using H_2PtCl_6 (0.1 g L^{-1} of Pt) as Pt source and urea (0.42 M) as the precipitating agent [1]. Other experimental parts are similar to synthesis of Cu-TiO_2. As shown in Fig. S7, photocatalytic H_2 production of Pt-TiO_2 is better than Cu-TiO_2 at same content of metal and the highest value is 8.91 mmol g^{-1} h^{-1} for Pt(2wt%)-TiO_2. However, it still lower than Cu(3%)-TiO_2/ErB-3mg (13.4 mmol g^{-1} h^{-1}), indicating that sensitization is an important method for improvement of photocatalytic ability. In addition, Pt is noble metal and its large-scale application would be limited.

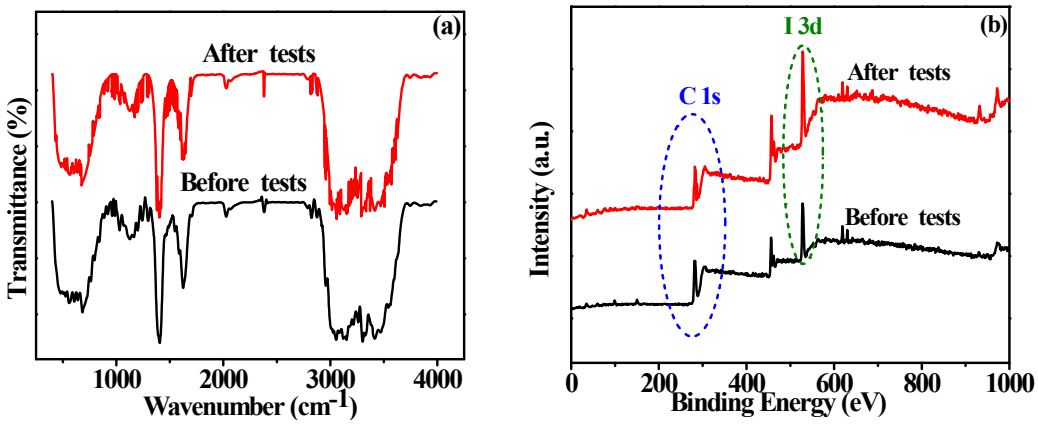

Figure S8 (a) FTIR spectra and **(b)** XPS spectra of Cu(3%)-TiO_2/ErB-3mg before and after cycling tests.

As shown in Fig. S8a, although some impurity peaks are observed, the main peaks of ErB still appear indicating the existence of ErB. Impurity peaks may attribute to fragments of ErB which degraded partly under irradiation. XPS spectra (Fig. S8b) show two new peaks which attribute to C 1s (marked by blue dashed line) and I 3d (marked by green dashed line). The new peaks attach to carbon and iodine elements of ErB.

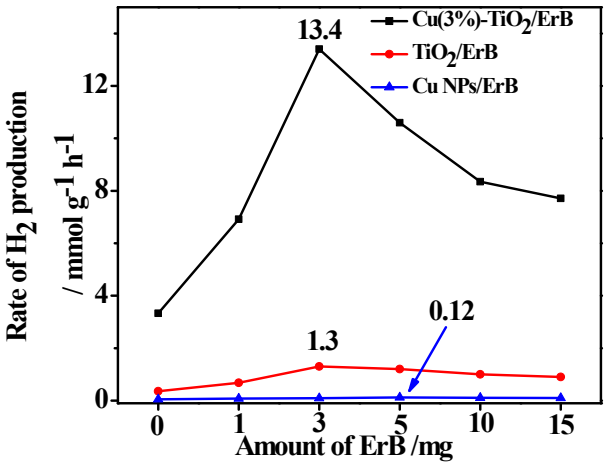

Figure S9 TiO_2, Cu NPs and Cu(3%)-TiO_2 photocatalytic H_2 production with sensitization by ErB under solar light irradiation.

Fig. S9 shows H_2 production rate of TiO_2 and Cu NPs sensitized by various amount of ErB. Cu NPs have a weak catalytic hydrogen production ability due to LSPR effect [2] and the rate of H_2 production is only 0.05 mmol g^{-1} h^{-1}, because electrons that induced by LSPR effect and then provided to H^+ is insufficient. After

sensitization, Cu NPs/ErB H_2 production increases but still keep at low level (0.12 mmol g^{-1} h^{-1}) due to lack of interaction with TiO_2. TiO_2 could be excited under solar light irradiation and used as a transfer station to promote electron transfer of photoinduction. In the absence of cocatalyst Cu NPs, H_2 production rate of TiO_2 is also low even sensitized by ErB (1.3 mmol g^{-1} h^{-1}). This result indicates charge transfer is inhabited without cocatalyst Cu NPs and recombination rate of electron-holes increases. From what have been discussed above, we can find that both single TiO_2 and Cu NPs are low active for H_2 production after sensitized by ErB. Therefore, the existences of TiO_2, Cu NPs and ErB are important for H_2 production in the catalytic system.

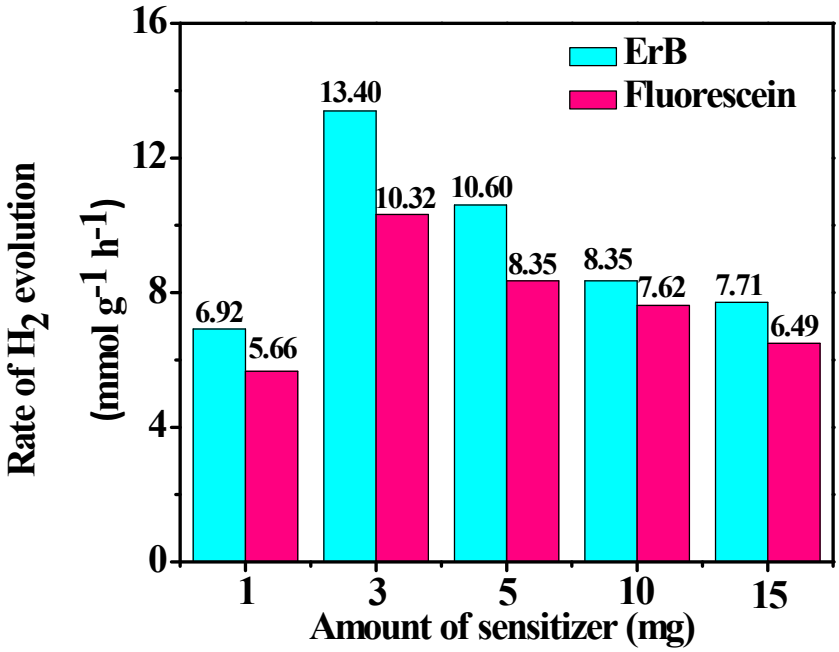

Figure S10 Photocatalytic H_2 production of Cu-TiO_2 with different sensitizer.

Hydrogen production of fluorescein (Aladdin Chemistry Co. Ltd.) sensitized Cu-TiO_2 was measured similar to ErB system. As shown in Fig. S10, hydrogen production of ErB system is slight higher than fluorescein system due to their different structures. Iodine is possible beneficial for photocatalysis.

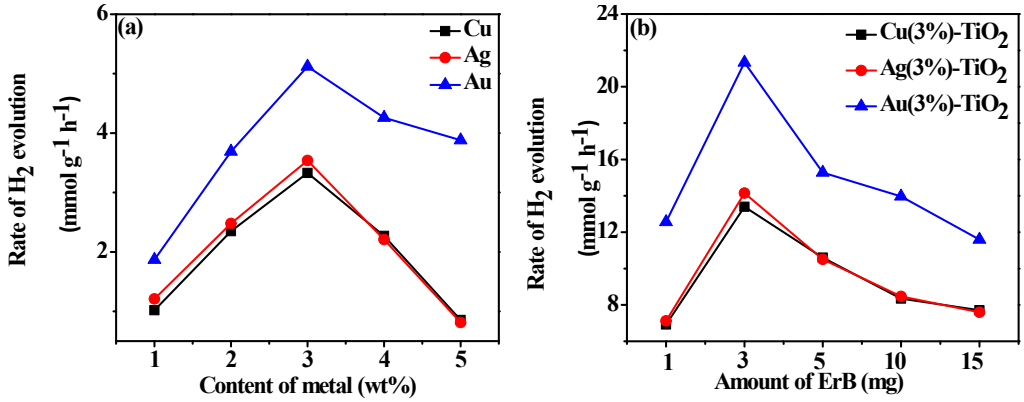

Figure S11 (a) Photocatalytic H_2 production of Metal-TiO_2 with various content of metal , **(b)** photocatalytic H_2 production of Metal(3%)-TiO_2 with different amount of ErB.

$AgNO_3$ and $HAuCl_4$ (Aladdin Chemistry Co. Ltd.) were used as precursor of metal nanoparticles and $NaBH_4$ solution was used as reductant. Other experimental sections are similar to synthesis of Cu-TiO_2. Au-TiO_2 and Ag-TiO_2 sensitization experiments are also similar to Cu-TiO_2.

As shown in Fig. S11a, photocatalytic H_2 production of Metal-TiO_2 order is Au>Ag≈Cu at the same content of metal and sensitization experimental results show same conclusion (Fig. S11b). In general, Au has the best catalytic effect in these three systems. Cu and Ag have similar catalytic effect. Au and Ag are noble metals and it is unsuitable for large-scale application, however, Cu is suitable for large-scale application in the future which deserves to further research.

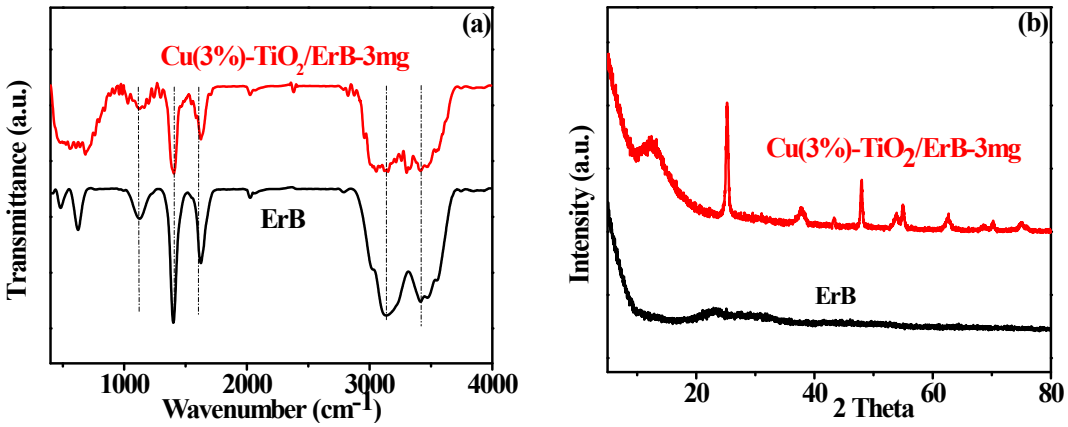

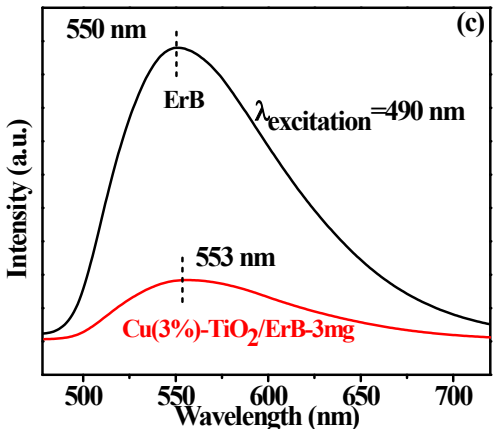

Figure S12 (a) FTIR spectra, **(b)** XRD patterns and **(c)** photo-luminescence (PL) spectra of ErB and Cu(3%)-TiO_2/ErB-3mg.

The Cu(3%)-TiO_2/ErB-3mg sample was obtained through centrifugation (10,000 rpm, 20 min) of reaction solution (contain 3 mg ErB) after irradiation 5 h. As shown in Fig. S12a, the FTIR spectra of ErB and Cu(3%)-TiO_2/ErB-3mg are similar from 1000 to 4000 cm^{-1} of wavenumber and this can be fully proved that the existence of ErB indicating that ErB dye molecules were absorbed on surface of Cu(3%)-TiO_2. There is a slight difference of peaks shape because of the interactions of ErB and Cu(3%)-TiO_2. The spectra of Cu(3%)- TiO_2/ErB-3mg at 400~1000 cm^{-1} have many differences due to existence of TiO_2 peaks. XRD patterns of Cu(3%)-TiO_2/ErB-3mg and ErB are shown in Fig. S12b. There is no obvious peak for ErB because of its amorphous phase. The intensity of peaks about Cu(3%)-TiO_2/ErB-3mg declines and the peak of Cu at 50.3˚ has disappeared, which can be attributed to the synergistic interactions of ErB and Cu(3%)-TiO_2. The photo-luminescence (PL) spectra (Fig. S12c) were investigated to evaluate the charge transfer from ErB to TiO_2. A strong emission peak at 550 nm is obtained on excitation at 490 nm with ErB, which is attributed to the electrons excitation from HOMO to LUMO of ErB under visible irradiation [3]. After sensitization by ErB, the emission peak exhibits an obvious decrease indicating electron transfer process should be enhanced. It is noteworthy that the peak of Cu(3%)-TiO_2/ErB-3mg shows small red shift from 550 to 553 nm because of Van Der Waals interactions of ErB and TiO_2 [3-5]. Van Der Waals interactions are very important for electron transfer from excited ErB to TiO_2. The above discussions

confirm that ErB dye molecules contact and exist synergistic interaction with Cu(3%)-TiO_2 and it is capable to sensitize Cu(3%)-TiO_2 efficiently.

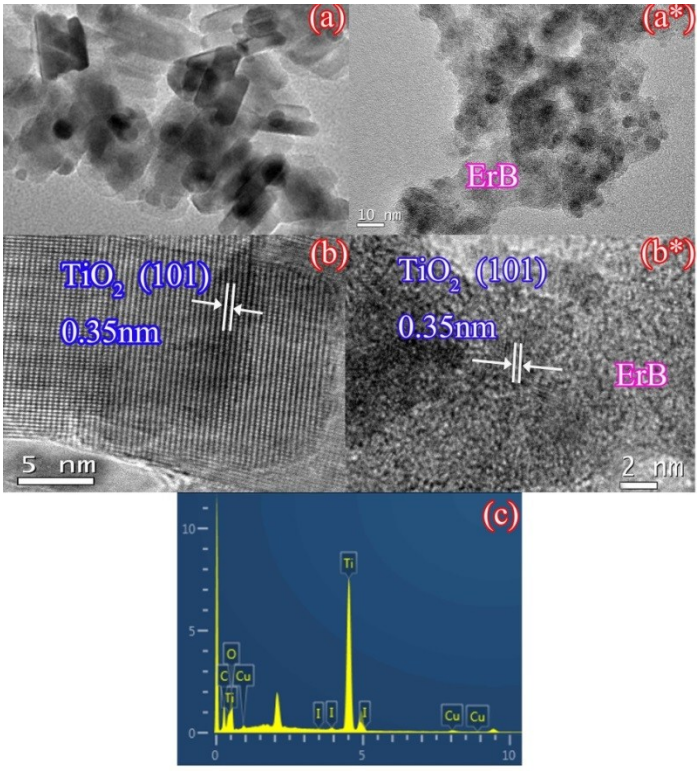

Figure S13 (a) TEM and **(b)** HRTEM images of Cu(3%)-TiO_2; **(a*)** TEM, **(b*)** HRTEM and **(c)** EDX spectrum images of Cu(3%)-TiO_2/ErB-3mg.

The low-magnification TEM image (Fig. S13a) shows the rod morphology of as-synthesized Cu(3%)-TiO_2 composites. After sensitization, the image (Fig. S13a*) becomes vague and cannot distinguish the shape of TiO_2 because of ErB cover. From the high-resolution TEM (HRTEM) image of Cu(3%)-TiO_2 (Fig. S13b), TiO_2 phase is clearly observed and the interlayer distance of 0.35 nm corresponds well with the lattice spacing of (101) plane of TiO_2. However, HRTEM image of Cu(3%)-TiO_2/ErB-3mg (Fig. S13b*) is also vague and only a few lattices are obtained due to TiO_2 phase. TEM images of Cu(3%)-TiO_2/ErB-3mg (Fig. S13a* and Fig. S13b*) are all vague illustrating that ErB is well absorbed on the surface of TiO_2 which dominates photocatalytic H_2 production. Fig. S13c is energy-dispersive X-ray spectroscopy (EDX) spectrum of Cu(3%)-TiO_2/ErB-3mg and it reveals existence of Ti, O, Cu, C, I. Carbon and iodine elements are found in the picture due to existence of ErB. This could also illustrate by XPS spectra (Fig. S8).

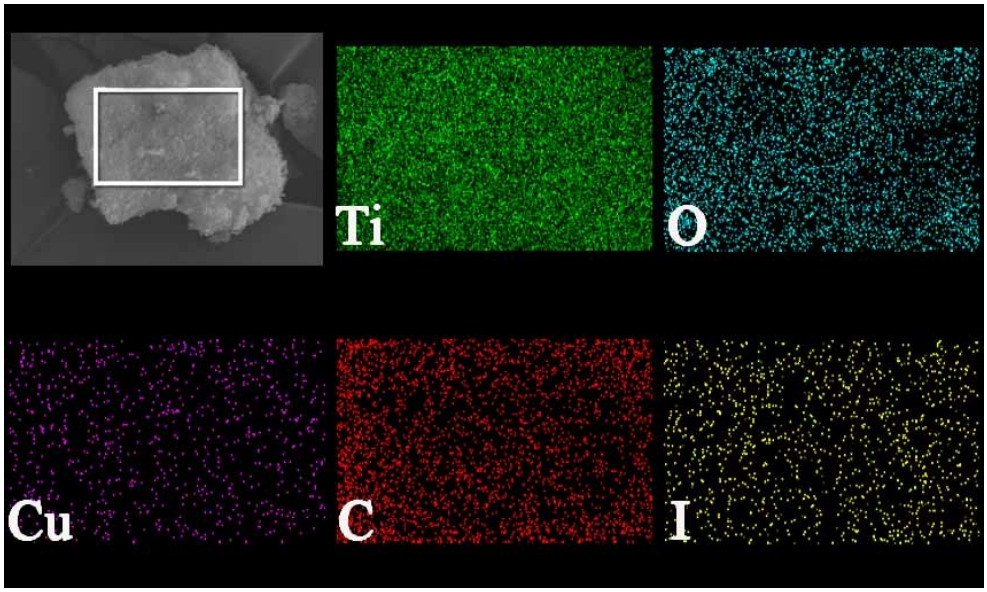

Figure S14 Elemental mapping patterns of Cu(3%)-TiO_2/ErB-3mg.

Table S1 Surface element composition of Cu(3%)-TiO_2 determined by XPS.

Sample	Elemental concentration (atom%)		
Cu(3%)-TiO_2	Ti 2p	O1s	Cu 2p
	31.91	66.27	1.82

Table S2 Surface element composition of Cu(3%)-TiO_2 before (1) and after (2) recycling photocatalytic reaction determined by XPS.

Sample	Elemental concentration (atom%)		
	Ti 2p	O1s	Cu 2p
1	31.91	66.27	1.82
2	30.23	68.16	1.61

Table S3 Adsorption amount of ErB.

Investment amount of ErB in experiment / mg	1	3	5	10	15
Adsorbtion amount of ErB / mg	0.1025	0.2018	0.2108	0.2201	0.2210

Adsorption amount of ErB increased with increase of ErB investment in experiment when investment amount of ErB under 5 mg. After investment amount of ErB more than 3 mg, adsorption amount of ErB increased not significantly or no increase, indicating adsorption of ErB reached saturation.

Table S4 Surface element composition of Cu(3%)-TiO_2/ErB-3mg before (1) and after (2) recycling tests determined by XPS.

Sample	Elemental concentration (atom%)				
	Ti 2p	O1s	Cu 2p	C 1s	I 3d
1	28.89	59.69	1.41	9.08	0.92
2	29.45	61.34	1.29	7.15	0.77

I 3d and C 1s have some decline due to photobleaching of ErB. Other elements have few differences.

Table S5 Apparent quantum efficiency (AQE) of photocatalysts [6].

Potocatalysts	Apparent quantum efficiency (AQE) %
TiO_2	0.221
Cu(1%)-TiO_2	0.657
Cu(2%)-TiO_2	1.235
Cu(3%)-TiO_2	2.315
Cu(4%)-TiO_2	1.427
Cu(5%)-TiO_2	0.492
Cu(3%)-TiO_2/ErB-1mg	3.216
Cu(3%)-TiO_2/ErB-3mg	4.673
Cu(3%)-TiO_2/ErB-5mg	3.981
Cu(3%)-TiO_2/ErB-10mg	3.652
Cu(3%)-TiO_2/ErB-15mg	3.335

The quantum efficiency is calculated from equation (1).

$$QE = \frac{2 \times the\ number\ of\ evolved\ H_2 molecules}{the\ number\ of\ incident\ photons\ (N)} \times 100\% \qquad (1)$$

N is determined by equation (2):

$$N = \frac{E\lambda}{hc}$$

Where E is the average intensity of irradiation which is determined by ILT 950 spectroradiometer (International Light Technologies), λ is wavelength, *h* is Planck constant and *c* is light speed.

References

[1] M.V. Dozzi, L. Prati, P. Canton and E. Selli, *Phys. Chem. Chem. Phys.*, 2009, **11**, 7171.

[2] J.P. Huo and H.P. Zeng, *J. Mater. Chem. A*, 2015, **3**, 6258.

[3] Z.Y. Li, Y.L. Fang, X.Q. Zhan and S.Xu, *J. Alloy Compd.*, 2013, **564**, 138.

[4] X. Wang, Q. Wang, F. Li, W. Yang, Y. Zhao, Y. Hao and S. Liu, *Chem. Eng. J.*, 2013, 234, 361.

[5] C. Pan, J. Xu, Y. Wang, D. Li and Y. Zhu, *Adv. Funct. Mater.*, 2012, **22**, 1518.

[6] J. Liu, Y. Liu, N. Liu, Y. Han, X. Zhang and H. Huang, Science, 2015, **347**, 970.